SACLANTCEN REPORT
serial no.: SR-155

SACLANT UNDERSEA
RESEARCH CENTRE

REPORT

Assimilation of hydrographic data from the Atlantic Inflow Experiment into ocean models

G. Peggion

October 1989

Page count for SR-155
(excluding covers)

Pages	Total
i–vi	6
1–17	17
@1–@15	15
	38

SACLANT Undersea Research Centre
Viale San Bartolomeo 400
19026 San Bartolomeo (SP), Italy

tel: 0187 540 111
telex: 271148 SACENT I

NORTH ATLANTIC TREATY ORGANIZATION

SACLANTCEN SR-155

Assimilation of hydrographic data from the Atlantic Inflow Experiment into ocean models

G. Peggion

The content of this document pertains to work performed under Project 04 of the SACLANTCEN Programme of Work. The document has been approved for release by The Director, SACLANTCEN.

Peter C. Wille
Director

intentionally blank page

Assimilation of hydrographic data from the Atlantic Inflow Experiment into ocean models

G. Peggion

Executive Summary: Forecasts of oceanic circulation phenomena to be useful in naval operational systems require a hierarchy of numerical models that describe the permanent features and predict the variability of the ocean dynamics. The ability of understanding the structure and dynamics of the ocean will improve acoustic propagation prediction. Central to this effort is the development of techniques to integrate into numerical models various types of environmental measurements which are distributed randomly in time and space and have differing error characteristics.

This report represents the link between the observational and numerical programs of the GIN Sea Project of SACLANTCEN. Hydrographic data are assimilated through a new procedure into 3D field distributions that can be used to initialise and update ocean circulation models. Most ocean circulation models start the computations by assuming the ocean to be at rest, requiring a large amount of computer time for the dynamics coming into balance. One way to increase the computational efficiency is to supply an initial velocity field compatible with the model formulation and the data distributions. From the processed temperature and salinity distributions, initial velocities are computed using the inverse method developed at the Centre.

Data from the GIN Sea '86 cruise of the Atlantic Inflow Experiment serve as prototype for the development of this technique. The resulting environmental conditions as derived for model initialization can be used directly for the analysis of the environmental conditions of the region. Comparison with the corresponding climatological distributions indicates the permanent features and the associated variability of the region of interest.

Further work will be directed towards the integration of the procedure into 3D time-dependent ocean dynamics models, and towards a similar analysis of other hydrographic data sets collected in the GIN Sea region.

intentionally blank page

Assimilation of hydrographic data from the Atlantic Inflow Experiment into ocean models

G. Peggion

Abstract: This study represents the link between observational and numerical programs. A method for data assimilation in dynamical analysis is presented and discussed. This approach assumes that the observational program furnishes an adequate 'instantaneous' representation of the ocean, but the region is lacking a large amount of historical data suitable for a valid analysis of the mesoscale variability.

From processed temperature and salinity distributions, absolute geostrophic velocities are computed using the inverse method proposed earlier by the author. The model is formulated on a 3D spherical-shell coordinate system, using geostrophic, hydrostatic, and Boussinesq approximations. Within the assigned dynamical constraints, a differential equation can be derived for the bottom pressure associated with the bottom geostrophic velocities. The results from the Atlantic Inflow Experiment are compared with climatological values from the Generalized Digital Environmental Model of the Naval Oceanographic Office.

Keywords: Atlantic Inflow Experiment ○ data assimilation ○ GIN Sea ○ objective analysis ○ oceanographic modelling

Contents

1

Introduction

The ocean is a complex geophysical fluid system with phenomena that occur on a broad range of space and time scales, and all of them may contribute significantly to the dynamics. The challenges of understanding and modelling such a system are amplified by the remoteness of the phenomena and the difficulty of acquiring timely data of sufficient high resolution. Thus, the choice of cut-off scale is often influenced by interest and practicability, rather than understanding and knowledge of the fundamental physical processes.

The ocean circulation was once thought to be a slow, large-scale flow. To this basic knowledge, mesoscale features have been recently inserted. Mesoscale variability, including features such as jet-like flows, rings, eddies, and front fluctuations are now known to be highly energetic and are considered to be dominant phenomena of the ocean circulation. Since oceanic mesoscale is an order of magnitude larger in period and smaller in space than its atmospheric counterpart (the synoptic scale), with adequate data assimilation and computational capability, realistic regional ocean forecasting could indeed be a reasonable goal.

Central to this technical approach is the coupling of the observations with numerical forecasting models, a relatively new task in physical oceanography, where with a few exceptions (Smith et al., 1985) typically modelers have constructed simulations and observers acquired and analyzed data, independently. Fitting data into models, usually requires assignement of estimated values to points of a regular net from the widely-spaced, irregularly-distributed observational grid of points. An ideal procedure would be to filter the noise inherent in the data without appreciable alteration of the field spectrum, and provide an 'exact' solution in regions which have not been sampled. To achieve this aim, it is not sufficient just to apply algorithms for a numerical interpolation; the resulting fields must also verify dynamical/statistical relationships which are known to be satisfied by the 'real' ocean.

Furthermore, in most of the numerical simulations, the momentum equations as well equations governing the density distribution (i.e. temperature and salinity equations) are integrated as an initial value problem usually starting from a state of rest. This requires the use of a large amount of computer time since the baroclinic adjustement time is of the order of a thousand years. In fact, most of the studies carry out initial computation for a few of hundred years of ocean time to allow the upper levels to come into approximate balance. To increase the computational efficiency of such numerical simulations, it is necessary to initialise the computations, supplying a

velocity field consistent with the mathematical formulation of the model and the initial data distributions. In this approach, a velocity field must be computed from a knowledge of the initial density distribution. This is a classical problem in physical oceanography. The solution obtained by the method proposed by Peggion (1987) is computed as a possible initial distribution for the circulation models that are under development at SACLANTCEN. The computer time required to reach the steady state from such a 'diagnostic' calculation is a small fraction of that required by the initial state of rest of the 'predictive' models mentioned above. Moreover, the initial configuration of the oceanic state may be used for the specification of open boundary conditions.

A reasonable compromise between the completeness of the model formulation and computational efficiency must usually be made for numerical models. Models that consider a broad range of dynamical balances are generally applied to limited regions of the ocean, which usually are not enclosed by coastlines, or rigid boundaries. Open boundaries are a difficult numerical task, and several techniques are available to avoid the region outside the numerical grid acting as a forcing for the inner regime. Predictive models with a limited forecasting range (with respect to the time-scale of the phenomena under investigation) may consider the initial value distributions fixed in time at the open boundaries. No appreciable alteration is introduced in the oceanic evolutionary state if the velocity field is coherent with the constituent distributions in the assumptions of the model formulation.

This report will address questions and present a method concerning optimal objective analysis schemes and optimal updating of initial/boundary conditions. Our approach has been suggested by two fundamental requirements: the use of simple mathematical algorithms and limited computer capabilities so that the whole procedure might be applied to understand in 'real' time (i.e. after the completion of the observational program) the oceanographic environmental conditions and associated circulation pattern.

The model is illustrated using data from the GIN Sea '86 cruise, the first hydrographic survey of the Atlantic Inflow Experiment (AIE), which is part of the GIN Sea Project of SACLANTCEN. The research objectives of the program are directed towards developing an extensive oceanographic information for the Greenland–Iceland–Norwegian (GIN) Sea. Although this basin has always attracted the attention of oceanographers, its geographical location made and makes work at sea difficult, so that the region is lacking a number of data and observations sufficient for an adequate analysis of its mesoscale variability. Thus, it is not possible to consider for the GIN Sea basin objective analysis methods based on statistical estimates such as the one described by Robinson (1986) and applied in regions extensively investigated such as the Gulf Stream region (Robinson and Leslie, 1985) and the Mediterranen Sea (Robinson et al., 1987). On the other hand, it is also expected that enough data and observations be collected during the GIN Sea program to avoid application of

objective analysis methods developed for situations in which data are too sparse to determine the state of a dynamical model (Bennett and May, 1987)

The estimates of regularly gridded constituent fields from irregularly scattered data sets is illustrated in Sect. 2. The circulation pattern relative to the data is presented in Sect. 3. The absolute geostrophic velocities are computed from observations of temperature and salinity fields. The results from the GIN Sea '86 cruise are compared with the velocity field derived using climatological data from the Generalized Digital Environmental Model (GDEM) of the Naval Oceanographic Office (NOO) in Sect. 4. Finally, Sect. 5 summarizes and discussed this research.

2

The treatment of data

The GIN Sea '86 experiment occupied 156 hydrographic stations between 26 May–30 June 1986 at the locations shown in Fig. 1. The measurements have been described and analyzed by Hopkins (1989). The AIE has been designed to provide information on the influx of the North Atlantic Water (NAW) that enters the GIN Sea from its southern boundary. Among the scientific questions addressed by the experiment, the program intends to determine the configuration, variability, and stability of the NAW boundary, and identify the associated large, and mesoscale features. Thus, although the records of the GIN Sea '86 cruise include signals in all the wavelength spectrum, it is possible to assume that the dominant features in the irregularly distributed data set are in the large-to-mesoscale range. Similarly, the records can be assumed to be simultaneous, since hydrographic surveys are usually on a time period of weeks, smaller than the mesoscale time scale, but large enough to filter small-scale variability.

Temperature and salinity data from the GIN Sea '86 cruise have been extracted from the environmental oceanographic database developed at SACLANTCEN for the Applied Oceanographic Group. In this oceanographic database, data are averaged 1 m in the vertical interval, but for the purposes of numerical model initialization, only 28 vertical levels are retained*. This data distribution contains two important features: there is a region of high point concentration (the Faeroe–Shetland Islands region), and a region of low-data density (the northern portion). The marked box in Fig. 1 represents the boundary of the regular mesh, which is defined on a 30×12 grid on the longitude and latitudes axes, corresponding to a spacing resolution of ca. 30 and 50 km, respectively.

Starting from the same features of the regular and irregular meshes, Peggion (1989) compared different interpolation algorithms and suggested new criteria to evaluate the accuracy of the solutions as functions of the dominant wavelength contained in the records. Since it is implicitly assumed that the records adequately describe the dominant scale features of the fields, in region of high point concentration the solutions from interpolation routines are accurate in their associated wavelengths. More difficult is the evaluation of the accuracy in region of low data-point concentration. Extrapolated large-scale solutions might be considered accurate because

* These levels are at depths of 0, 30, 50, 75, 100, 125, 150, 200, 250, 300, 400, 500, 600, 700, 800, 900, 1000, 1100, 1200, 1300, 1400, 1500, 1750, 2000, 2800, 3200, 3400 from the sea surface.

synoptic features are resolved by many points of both regular and irregular grid. On the other hand, extrapolated solutions in the mesoscale range are of low reliability because the regions lacking data are greater in dimension than that of the features under investigation. Thus, solutions with mesoscale features must be constrained to physical/statistical relationships, in region which have not been sampled.

Without a large number of historical data sets suitable for a correct application of statistical methods, there are several ways in which new information might be supplemented by prior knowlegde or prejudice. One possibility is simply to require the extrapolated solution be sufficiently smooth in a variational framework in which a cost function, measuring model data misfit, is minimized (Sasaki, 1970; Thacker, 1986). In the recent years, assimilation of satellite data into ocean models has also been considered. However, the problem of using surface observations to determine the deeper structure of the ocean has not been completely investigated (Webb and Moore, 1986). Another approach would be the use of climatological models and introduce in regions lacking records bogus data which would be treated as real when interpolation is performed (Thacker, 1988). Although there would not be relationships between climatological values and temporal evolution of the system, the bogus data would have at least the correct order of magnitude, and climatological covariance would help to ensure a certain degree of smoothness, while coupling the two different sets.

In the following experiments, we will require that far from the data points, the fields be climatological. More specifically, outside the envelop of the station locations, bogus data are assigned from the GDEM model. GDEM is a 4D, steady-state model of ocean temperature and salinity in which seasonal data are stored with a grid spacing of 30-arc minutes at 30 vertical levels (Davis et al., 1985). Considering the time period in which GIN Sea '86 took place, the added data are the averaged values of spring and summer seasons. Tests have been made to control the dependence of the solution on the extension of the climatological region. It has been found that the solution is not particularly affected by the location of the bogus data, if they lie outside the envelop of the reporting points. The regions outside the dashed lines in Fig. 1 represent the areas in which bogus points have been added. Extrapolation/interpolation is not extended to the shallow channel between Norway and the Shetland Islands. As will be discussed later, the model formulation for computing the absolute velocities ignores physical processes intrinsic to the dynamics of coastal waters.

Finally a few remarks on the vertical structure of the field distributions. The mesoscale variability of the ocean tends to be concentrated in the upper surface layer where there are large velocity and density gradients and atmospheric fluctuations most likely generate ripples and meanderings of the zonal fronts. Below the main thermocline, the circulation pattern exhibits slower current systems with lesser spatial and temporal excursions. These general features suggest a treatment of the data based on two different numerical procedures. The first algorithm produces a

solution which is accurate in the mesoscale wavelength, and adequate for the field distributions of the upper layer. Interpolation is performed over the set of data points given by both original records and climatological bogus values, using the ZGRID(10) routine (Taylor et al., 1971). The second algorithm produces a solution which preserves the large-scale features contained in the records, and is appropriate for the field distribution of the deep ocean. The numerical procedures interpolates only over the original reporting points, using the GKRIG2 routine (UNIRAS, 1986). The accuracy and validity of the method have been tested in a previous work (Peggion, 1989).

To guarantee a smooth transaction between the upper and deep water solutions, the two algorithms are blended together in a depth function. Let $I_Z(k)$ and $I_G(k)$ be the interpolated solution at depth d_k obtained by ZGRID(10) and GKRIG2 routines, respectively. Let D_0 be a reference depth (the value $D_0 = 1100$ m is henceforth considered), thus the interpolated solution, $I(k)$ is defined as follows:

$$I(k) = \begin{cases} (1-\alpha_k)I_Z(k) + \alpha_k I_G(k), & d_k \leq D_0 \\ I_G(k), & d_k > D_0, \end{cases}$$

where $\alpha_k = \xi_k^2 e^{(1-\xi_k^2)}$ is a weighting coefficient, and $\xi_k = d_k/D_0$ a dimensionless variable of depth. The definitions of the coefficient α_k and reference depth D_0 are arbitrary. However, this choice concentrates the mesoscale features above the thermocline depth (more than 50% of the solution in the upper 800 m is from the ZGRID algorithm) and guarantees a smooth transaction between the two numerical procedures.

The solutions at 30 m ($\alpha_{30} = 4.7 \times 10^{-3}$), and 500 m ($\alpha_{500} = 0.30$) depth are illustrated in Figs. 2 and 3, respectively. Density distribution is computed from temperature, salinity and depth values using the UNESCO '80 equation of state (Millero and Poisson, 1981). The influence of the bogus data upon the solutions is easily observable. On the northwestern portion of the domain, the climatological data suggest the presence of the Icelandic Front, which was not not sampled by the hydrographic survey at the upper levels. This front, which defines the southern penetration of the Arctic Water (ArW) in the region, presents surface manifestations highly variable in space and time. At greater depths the front moves southwards, but its location is more stable, with lesser excursions (Hopkins, 1988). Although climatology could never reproduce 'realistic' position and shape of the front, the bogus data contribute important information pertaining to the physics and dynamics of the region. The 'unrealistic' reproduction of the front appers more evident in the upper levels of the ocean, where the front variability implies a climatological configuration wider and weaker than its temporal evolution. At greater depths the front has moved southwards, but its location is defined by both original records and climatological values.

Two vertical sections of the constituent distributions are depicted in Figs. 4a–d. The section at 61.5°N contains values only from the survey itself, indicating the

NAW which flows northwards in the Faeroe–Shetland Channel. The northern section includes original records in its central part, and bogus data on the both western and eastern sides. At these latitudes, the records from the two northern transects of the GIN Sea '86 cruise separate fairly well the NAW and ArW masses whose locations are suggested by the climatological values. Finally, both vertical sections confirm a smooth transaction between the $I_Z(k)$, and the $I_G(k)$ solutions.

3

The circulation pattern

3.1. THE INVERSE METHOD

A complete description of the model formulation is given by Peggion (1987). In this procedure the ocean is assumed to be non-diffusive, hydrostatic and incompressible, and the flow geostrophic and inviscid. The problem may be formulated as follows: Given the density distribution ρ, find the velocity (u, v, w) and pressure p which satisfy the equations

$$-fv = -\frac{1}{\rho_0 r \cos\phi} p_\lambda, \tag{3.1a}$$

$$fu = -\frac{1}{\rho_0 r} p_\phi, \tag{3.1b}$$

$$0 = -p_z - g\rho, \tag{3.1c}$$

$$\frac{1}{r\cos\phi}\left(u_\lambda + (\cos\phi v)_\phi\right) + w_z = 0, \tag{3.1d}$$

$$f = 2\Omega \sin\phi. \tag{3.1e}$$

The equations are referred to a spherical-shell coordinate system (ϕ, λ, z) where ϕ is the latitude, λ the longitude, and the vertical coordinate z is zero at a bottom reference level and increases upwards. The subscripts ϕ, λ, and z denote partial differentation, $u = r\cos\phi\dot{\lambda}$ is the eastward velocity, $v = r\dot{\phi}$ the poleward velocity, and w the vertical velocity. The constant r is the radius of the earth, ρ_0 a constant reference density, f the Coriolis parameter, g the gravitational acceleration assumed constant, and Ω the angular speed of rotation of the earth. The bottom of the ocean is taken to be at $z = h(\lambda, \phi)$, and the mean sea-surface displacement at the reference level $z = H$. Equations (3.1a–e) are satisfied in the domain $V = \{\phi_0 \leq \phi \leq \phi_1,\ \lambda_0 \leq \lambda \leq \lambda_1,\ h \leq z \leq H\}$.

Integration of the hydrostatic equation (3.1c) from the ocean bottom to a depth z,

$$p(\lambda, \phi, z) = -g \int_h^z \rho(\lambda, \phi, z)\, \mathrm{d}z + p_\mathrm{b},$$

introduces p_b which is an unknown function of (λ, ϕ) and cannot be determined from the dynamics (3.1) alone. The indeterminacy in the pressure entiles a similar indeterminacy in the velocity field. Following the classical formulation of this inverse

problem (Wunsch, 1978; Fiadeiro and Veronis, 1982) extra information in the form of the density equation

$$\frac{1}{r\cos\phi}\,u\rho_\lambda + \frac{1}{r}v\rho_\phi + w\rho_z = 0, \tag{3.2}$$

is usually added. Although geostrophic and hydrostatic approximations do not restrict p_b, a given density distribution ρ may satisfy Eq. (3.2), but could be not compatible with the dynamics (3.1). Franzen and Warn-Varnas (1988) presented the mathematical conditions that a given function must verify to be a density distribution coherent with Eqs. (3.1) and (3.2).

Despite the rigour of this mathematical theorem, it is not implied that an observed density distribution satisfy these conditions. A 'true' observed density field contains noise in the measurements of temperature and salinity distributions, and errors due to the model formulation (3.1) ignoring terms that might be dynamically important. The consequent misfit in Eq. (3.2), which is never assumed to be zero, is an additional unknown of the problem. Here, it is defined solution the bottom pressure p_b and its associated geostrophic bottom velocities that minimize the variance of the misfit in the domain V, consistently with the data, and the assigned dynamics (3.1).

3.2. THE ABSOLUTE VELOCITIES

In this section the method of Subsect. 3.1 is applied to the data collected during the AIE, and processed as described in Sect. 2. Figures 5a–d summarize the solution resulting from the inversion which reflects the generally accepted picture of this region of the GIN Sea basin. Two main circulation systems can be easily identified. From the northwestern corner of the domain, water of arctic origin (ArW) proceeds southwards and impinges the northern side of the Faeroe Continental Shelf. From the Faeroe–Shetland Channel (FSC), the NAW enters the GIN Sea and moves northwards following approximately the 800 m isobath of the Norwegian Continental Shelf. This circulation system is usually known as the Norwegian Atlantic Current (NwAtC). At the eastern boundary of the domain, the solution also shows evidence of a second branch of this current system flowing northwards along the Norwegian coast, mainly induced by the coastal salinity front which appears clearly in Fig. 2c.

The different origin of the NAW and ArW masses makes their detection easy, although mixing and diffusive processes and air/sea interactions may modify their intrinsic characteristics. With respect to this solution, NAW is warm and of high salinity with surface values of temperature $T > 8.5°$ and salinity $S > 35.15$ ppt; ArW is cold and of low salinity with surface values $T < 5.5°$ and $S < 35$ ppt. These values imply that the surface eastern boundary of the NwAtC is along the $\sigma_t = 27.4$ isopycnal, where both velocity and constituent distributions present evidence of meandering and small eddies.

ArW mainly occupies the western side of the domain and the associated velocities are mostly barotropic with weak vertical shear. When ArW flows along the northern side of the Faeroe Continental Shelf, most of this flow recirculates back into the Norwegian Sea, but a small part of it moves southwards into the FSC along the Faeroe side. From the FSC the surface ArW can leave the GIN Sea basin, but at greater depths ArW is reflected backwards by the topography of the area. Although this description is coherent with the solution obtained by the inversion, the sampling interval and numerical grid resolution may not be adequate to describe the full circulation system along the Faeroe Continental Shelf. Hopkins and Mouchet (personal communication) suggested that NAW flowing from the North Atlantic Ocean impinges the Faeroe Continental Shelf and splits into two branches: one into the FSC, the other over the Iceland–Faeroe Ridge (IFR). While the flow into the FSC proceeds northwards carrying most of the NAW transport; the flow over the IFR may recirculate backwards, after having lost some heat and salt by diffusion to the surrounding colder and fresher waters. This circulation system creates a region of high small variability, where the present analysis might not apply correctly. Although the secondary inflow of NAW over the IFR is not well resolved in the velocity field distribution, the existence of this branch is also supported by Fig. 3b where an intrusion of saltier water over the IFR is clearly noticeable.

Two longitudinal velocity sections are depicted in Figs. 6a and b, illustrating the changes and transformations of the NwAtC as it proceeds northwards. Constrained by the topography of the FSC, at the lowest latitude, the NAW moves as a strong, narrow, jet-like flow. The computations indicated a width of about 225 km and a transport of ca. 3.3 Sv, with maximum velocity values of about 10 cm/s. It is also important to consider the vertical extension of the NwAtC: velocities greater than 1 cm/s are found in a region of maximum thickness of 500 m, whose boundary might be identified with the 4° isotherm. Inside this area, the velocity field presents a stronger vertical shear, indicating that the circulation is mainly baroclinic.

At the highest latitude, the NwAtC has spread in a wider shallower current with a transport of ca. 3.6 Sv. Velocities greater than 1 cm/s are still enclosed by the 4° isotherm, which can be considered a good signal for the NAW. Inside this isotherm, the velocity experiences a weaker vertical shear, indicating that mixing and diffusive processes have reduced the baroclinicity of the NwAtC. Table 1 summarizes the values relative to the two sections. Values are reported for the northward and southward flow, separately, to avoid arbitrary numerical criteria for the definition of NAW and ArW masses. However, at lower latitudes the northward flow can be identified with the inflow of NAW, but at higher latitudes it also includes recirculation of ArW. Since the domain of interest has open boundaries, width and thickness of the southward flow are not computed.

Figure 6b confirms the presence of a cold eddy at the western edge of the NAW. As was discussed in Sect. 2, values at 64°N are mostly climatological, with data from the AIE only at the middle longitudes. Although the constituent distributions

Table 1
The Atlantic Inflow Experiment

Section	Transport (Sv)	Max. velocity (cm/s)	Width (km)	Thickness (m)
Northward flow				
61.5°N	3.3	10	225	500
64.0°N	3.6	7	390	300
Southward flow				
61.5°N	1.6	4	–	–
64.0°N	5.0	4	–	–

appeared smooth and 'realiable' enough, there is no guarantee the solution is 'truly' representative of the dynamical oceanographic conditions during the AIE, and the eddy present in the solution may not have been there. Even though the eddy is in the region where the hydrographic stations have been located, the 'true' oceanic distribution might assume a completely different configuration. Without additional information, we can only affirm that according to the current state of knowledge, the eddy is the most 'probable' solution in which mesoscale variability dominates.

4

The climatological distribution

In this section, the inverse method described in Subsect. 3.1 is applied in the same region of the AIE, applying the climatological temperature and salinity distributions from GDEM. This model is derived using an interpolated temporal and spatial grid of spline coefficients of 1D functional form, rather than interpolated values of measured profiles at selected depths. Figures 7 and 8 illustrated the climatological conditions computed as the averaged values of the spring and summer seasons. Comparison with the AIE observational data sets indicates that climatological values do not reproduce the mesoscale features described in the previous section (henceforth referred to the evolutionary state) adequately. Because of the high spatial and temporal variability of the NwAtC, the averaging processes in the GDEM procedure tend to result in an over-smoothed image of the environmental conditions which does not compare to the observations. Climatological constituent distributions are smoother with weaker horizontal gradients. Fronts and other mesoscale features are poorly reproduced at all depths (Fig. 9); only the climatological salinity front along the Norwegian coast is stronger than that measured during AIE.

The environmental conditions derived from GDEM constituent distributions are shown in Fig. 10. They indicate the effects of both mesoscale variability and climatological processes of the observational data, and how these two factors interact and contribute in different forms. In the proximity of the FSC, the GDEM regular mesh resolution is too coarse with respect to the width of the channel. This poor resolution averages the lateral excursions of the NAW boundary into a smooth climatological distribution, so that the dynamics of the Atlantic inflow cannot be reproduced within an acceptable degree of accuracy. ArW flowing outside the FSC region is less affected by the coarse grid resolution, and being more uniform and homogeneous than NAW is less sensible to climatological smoothing. At higher latitudes, the fluctuations of the front, and the climatologiacal processing of the observation do not result in a smooth transition between the NAW and ArW masses, but suggests the presence of several weak fronts at different locations so that the associated flow is composed of a system of narrow poleward and southward jet-like currents, extending all over the water column (Fig. 11). Numerical tests have been made to guarantee that the solution is not a consequence of averaging over two seasonal values. Similar velocity fields have been obtained from spring and summer constituent distributions, separately.

Comparison with the solution obtained from the AIE observational data indicates that climatological and evolutionary states have similar trends and configurations.

Both circulation systems present a southward flow along the north side of the Faeroe Continental Shelf which appears to be reflected backwards into the GIN Sea basin along the edge of an anticyclonic gyre. The limits and validity of such an explanation were discussed in Sect. 3. Similarly to the environmental conditions of the AIE, the climatological data also show a weak sign of an intrusion of saltier water from the IFR. Thus, this inflow of NAW over IFR may be considered a permanent feature of the region, although with high spatial and temporal fluctuations.

Both evolutionary and climatological solutions simulate the NwAtC, but meandering, small eddies, and other equivalent mesoscale features are swept away from the GDEM solution. The two solutions differ mostly in the values of the associated currents and transports, as shown in Table 2. With the exception of the FSC region, where the dynamics is poorly approximated, the climatological circulation of NAW presents smaller surface velocities, but a greater local transport. Moreover, the climatological poleward flow penetrates at great depths, while the relative evolutionary flow is confined in the upper 500 m of the water column. These signals indicate a weaker vertical shear and therefore the climatological configuration of the NwAtC is less affected by the thermohaline balance. On the other hand, the circulation system of ArW derived from GDEM data is generally overestimated and presents stronger surface velocities and higher local transport values. The vertical structure does not show evidence of strong vertical shears, so that climatological conditions empahasize the barotropic regime of ArW.

Table 2
Climatological values

Section	Transport (Sv)	Max. velocity (cm/s)	Width (km)	Thickness (m)
Northward flow				
61.5°N	0.6	2.0	260	500
64.0°N	5.7	6.4	380	1500
Southward flow				
61.5°N	3.7	6.3	–	–
64.0°N	9.0	5.6	–	–

5
Conclusions

This study represents the link between the observational and numerical programs of the GIN Sea project of SACLANTCEN. Numerical models usually require initial knowledge of density (i.e. temperature and salinity) distributions and velocity field. To increase the computational efficiency of the code, a velocity field coherent with the mathematical formulation of the model needs to be assigned. Both physical and dynamical field distributions have been computed and analysed. Data from the GIN Sea '86 cruise of the AIE have served as prototype for the development of this procedure for fitting data into model initialization.

Observational data have been processed starting from the following assumption: knowledge of the GIN Sea region is too limited for developing statistical method, but not too scarce for application of methods based on a prior prejudice of the field distributions. It is implicitly assumed that the observational program furnishes adequate information to determine the 'instantaneous' configuration of the ocean, but is unable to determine anomalies of the field with respect to a 'standard' state. An objective analysis procedure is proposed to provide a 3D ocean structure which preserves the dominant spatial features contained in the records. Since the AIE program intends to determine synoptic and mesoscale features of the influx of NAW, data are processed so that mesoscale variability dominates the upper levels of the ocean, and large-scale features the deep strata. In regions lacking observational data, the fields are costrained to be climatological. Although climatology does not represent the most probable 'instantaneous' configuration, but minimizes the deviation of anomalous states, the added bogus data preserve the correct order of magnitude of the measured values.

From the processed data distributions, absolute velocities have been computed. The model formulation assumes the ocean to be inviscid and non-diffusive and the flow geostrophic and hydrostatic. The assumptions of geostrophic and hydrostatic balance are traditional and often confirmed by measurements taken in the inner ocean. The omissions of the influence of the relative vorticity, and boundary layer activities are the major limitations of the method. The solutions of the inversion are obtained in a mathematical framework that implicitly assumes that the barotropic component of the velocity field has a length scale large with respect to the station grid, and the small-scale noise in the hydrographic data is uncorrelated between stations (Peggion, 1987). The consequences of such an assumption are evident: the evolutionary and climatological solutions are quite different even in the northern part of the domain, where GDEM climatological data dominate in both constituent distributions.

The resulting environmental conditions as derived for model initialization, can be used directly for the analysis of the region. Comparison with the correspondent climatological distributions indicates the permanent features of the fields and their variability. The region of AIE is characterized by the inflow of NAW through the FSC. The 500-m sill depth of the channel does not inhibit the water input, and NAW moves northwards approximately along the 800 m isobath of the Norwegian Continental Shelf. NAW proceeds inside the GIN Sea basin as a compact mass of water with only limited vertical and horizontal exchanges of salt and heat with the surrounding ArW. These conditions create a strong front between the two water masses. The front is characteristically dynamically unstable with the development of meanderings and small eddies. Moreover, NAW results high variable in space and time and under baroclinic regime, with strong vertical shear of the velocity profiles. ArW, being more uniform and homogeneous, has a more marked barotropic circulation system, suggesting that wind and other atmospheric forcing could be the main driven mechanisms. The absence of mixed-layer dynamics in the model formulation of the inverse problem could imply that the dynamics of ArW is not as well represented as that of NAW. However, Holland and Hirschman (1972) indicated that in diagnostic computations (i.e. density field is known) wind stress is unimportant because the density field carries most of the information about the long-term wind forcing.

The differences between climatological and evolutionary state reflect also the sensitivity of the procedure to the constitient field distributions. Climatological processing smoothes the lateral variations of the fields, and emphasizes the barotropic component of the circulation system. In the AIE region of interest, climatology could underestimate the NAW flow, which in the evolutionary case has been found under baroclinic regime, but overestimate the ArW circulation which has been already found to be barotropic. At the present stage of this investigation it is not possible to define quantitavely the errors in the solutions. The evolutionary and climatological states as illustrated in this study are consistent with the approximations and assumptions made along the development of this procedure, but cannot represent the 'real' environmental conditions.

References

[1] Bennett, T. and May, P. An optimal thermal analysis for the naval oceanography program. NORDA Report. NSTL Station, MS, Naval Ocean Research and Development Activity, 1977.

[2] Davis, T.M., Countryman, K.A. and Carron, M.J. Tailored acoustic products utilizing the NAVOCEANO GDEM (a Generalized Digital Environmental Model). 36th US Naval symposium on underwater acoustics. San Diego, 1–3 April 1985.

[3] Fiadeiro, M.E. and Veronis, G. On the determination of absolute velocities in the ocean. *Journal of Marine Research*, **40**, (supplement) 1982: 159–182.

[4] Frenzen, C.L. and Warn-Varnas, A.C. Implications of conservation equations for the determination of absolute velocities. *Journal of Marine Research*, **46**, 1988: pp. 701–714.

[5] Holland, W.R. and Hirschman, A.D. A numerical calculation of the circulation in the North Atlantic Ocean. *Journal of Physical Oceanography*, **2**, 1972: 336–356.

[6] Hopkins, T.S. The GIN Sea. Review of physical oceanography and literature from 1972, SACLANTCEN SR-124. La Spezia, Italy. SACLANT Undersea Research Centre, 1988.

[7] Hopkins, T.S. Atlantic Inflow Experiment, GIN Sea Cruise '86 – Data Report – Part I: Hydrography, SACLANTCEN SM-209. La Spezia, Italy. SACLANT Undersea Research Centre, 1989.

[8] Millero, F.C. and Poisson, A. International one-atmosphere equation of state of seawater. *Deep-Sea Research*, **27A**, 1981: 255–264.

[9] Peggion, G. A method for determining absolute velocities from hydrographic data, SACLANTCEN SR-114. La Spezia, Italy, SACLANT Undersea Research Centre, 1987. [AD B 117 448]

[10] Peggion, G. Test and evaluation of objective mapping applied to oceanographic data from GIN Sea '86, SACLANTCEN SM-217. La Spezia, Italy, SACLANT Undersea Research Centre, 1989. [AD B 132 964]

[11] Robinson, A.R. Data assimilation, mesoscale dynamics and dynamical forecasting. *In*: O'Brien, J.J. *ed.* Advanced Physical Oceanographic Numerical Modelling, Dordrecht, the Netherlands, Reidel, 1986: pp. 465–483.

[12] Robinson, A.R., Hecht, A., Pinardi, N., Bishop, J., Leslie, W.G., Rosentroub, Z., Mariano, A.J. and Brenner, S. Small/synoptic mesoscale eddies. The energetic variability of the Eastern Levantine Basin. *Nature*, **327**, 1987: 131–134.

[13] Robinson, A.R. and Leslie, W.G. Estimation and prediction of oceanic fields. *Progress in Oceanography*, **14**, 1985: 485–510.

[14] Sasaki, Y. Some basic formalisms in numerical variational analysis. *Monthly Weather Review*, **98**, 1970: 875–883.

[15] Smith, J.A., Mooers, C.N.K. and Robinson, A.R. Estimation of quasi-geostrophic model amplitudes from XBT/CDT survey data. *Journal of Atmospheric and Oceanic Technology*, **24**, 1985: 491–507.

[16] Taylor, J., Richards, P. and Halstead, R. Computer routines for surfaces generation and display, Manuscript Report Series, 16. Ottawa, Canada, Department of Energy, Mines and Resources, Marine Sciences Branch, 1971.

[17] Thacker, W.C. Relationships between statistical and deterministic methods of data assimilation. *In*: Sasaki, Y.J. *ed.* Variational methods in the Geosciences. Amsterdam, Elsevier, 1986: pp. 173–179.

[18] Thacker, W.C. Fitting models of inadequate data by enforcing spatial and temporal smoothness. *Journal of Geophysical Research*, **93**, 1988: 10655–10665.

[19] UNIRAS. Reference Manuals, Version 5. Lynbgy, Denmark, UNIRAS, 1986.

[20] Webb, D.J. and Moore, A. Assimilation of altimetry data into ocean models. *Journal of Physical Oceanography*, **16**, 1986: 1901–1913.

[21] Wunsch, C. North Atlantic general circulation west of 50°W determined by inverse methods. *Review of Geophysics*, **16**, 1978: 583–620.

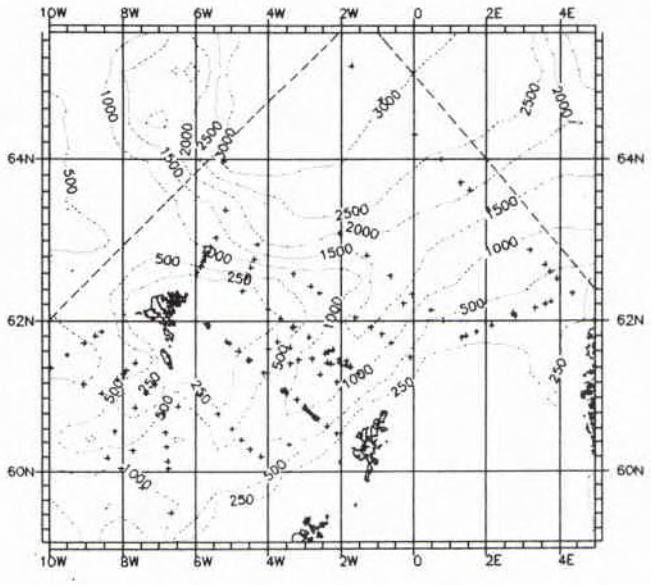

Fig. 1. GIN Sea '86 cruise data distribution. The dots represent CTD cast stations. The regions outside the dashed lines represent the areas where climatological bogus data have been added.

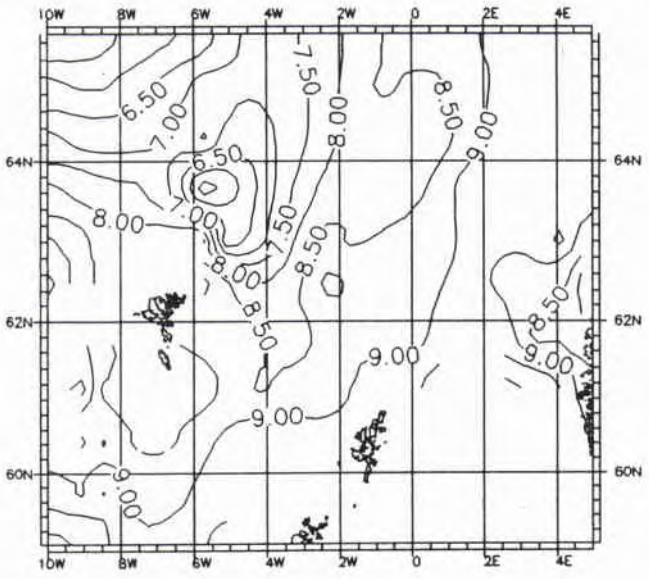

Fig. 2a. **The constituent distributions at 30 m depth during AIE: Temperature (contour interval $\Delta T = 0.5°$).**

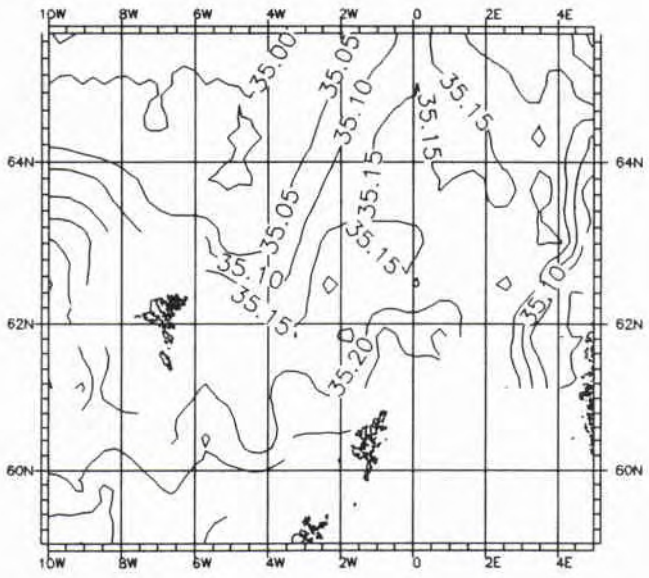

Fig. 2b. **The constituent distributions at 30 m depth during AIE: Salinity (contour interval $\Delta S = 0.05$ ppt).**

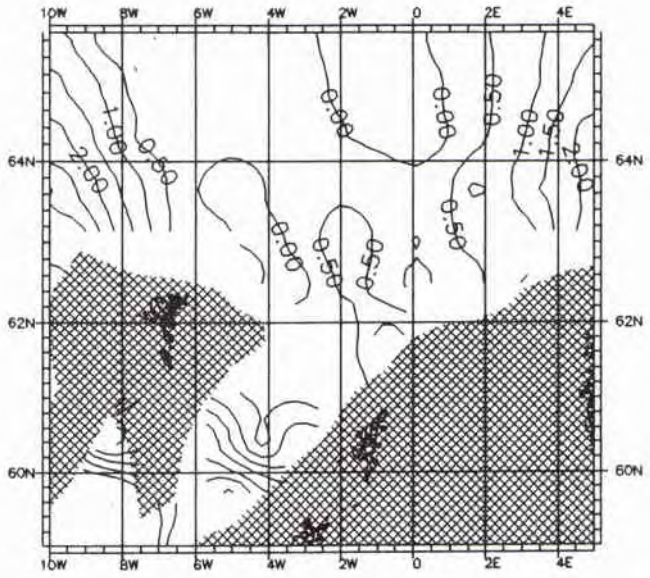

Fig. 3a. **The constituent distributions at 500 m depth during AIE: Temperature ($\Delta T = 0.5°$).**

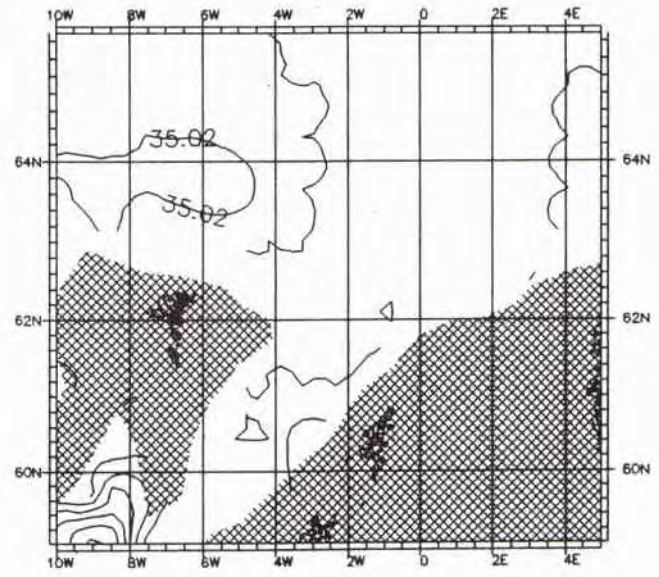

Fig. 3b. **The constituent distributions at 500 m depth during AIE: Salinity ($\Delta S = 0.02$ ppt).**

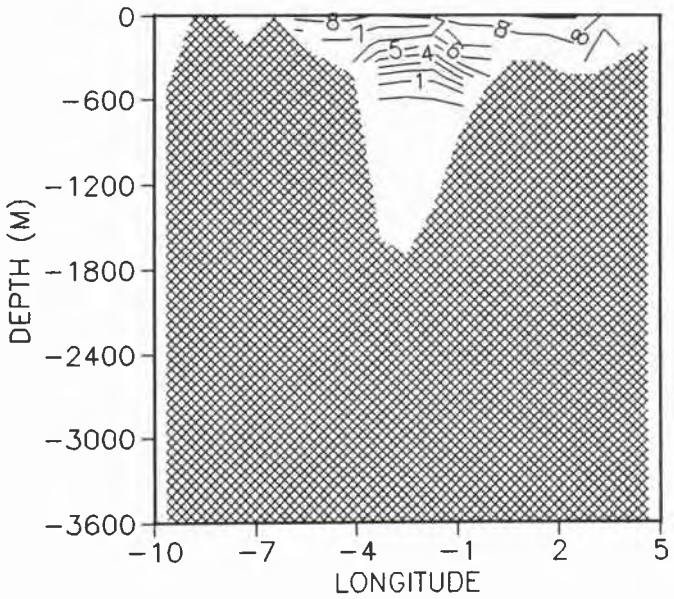

Fig. 4a. **Two longitudinal sections during AIE: Temperature at 61.5°N ($\Delta T = 1°$).**

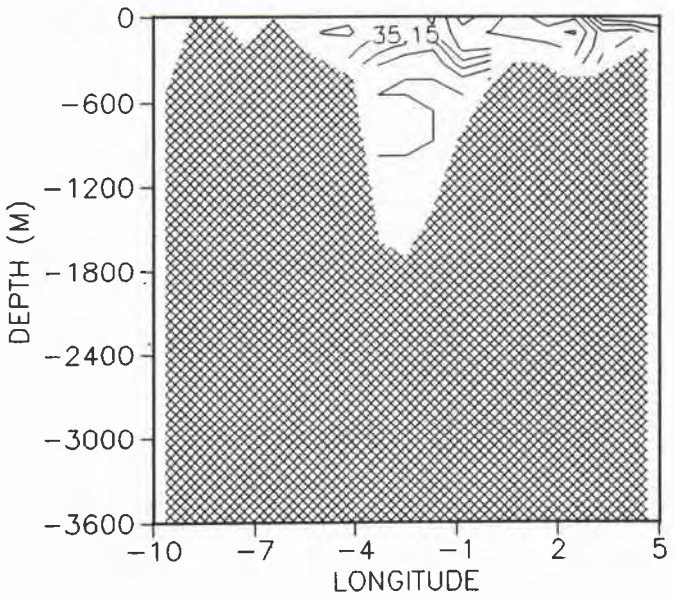

Fig. 4b. **Two longitudinal sections during AIE: Salinity at 61.5°N ($\Delta S = 0.05$ ppt).**

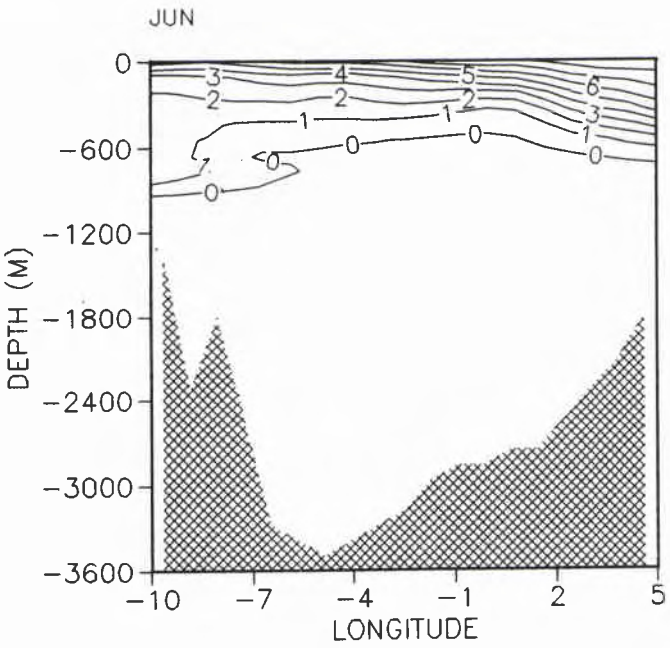

Fig. 4c. **Two longitudinal sections during AIE: Temperature at 64°N ($\Delta T = 1°$).**

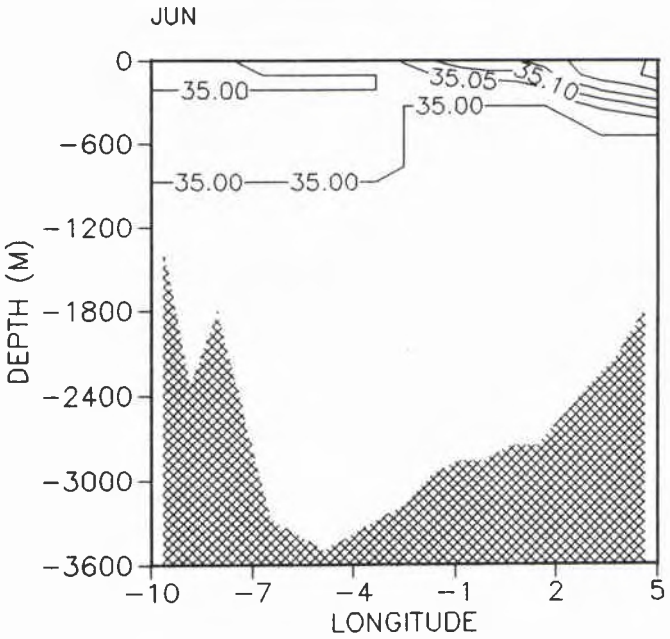

Fig. 4d. **Two longitudinal sections during AIE: Salinity at 64°N ($\Delta S = 0.05$ ppt).**

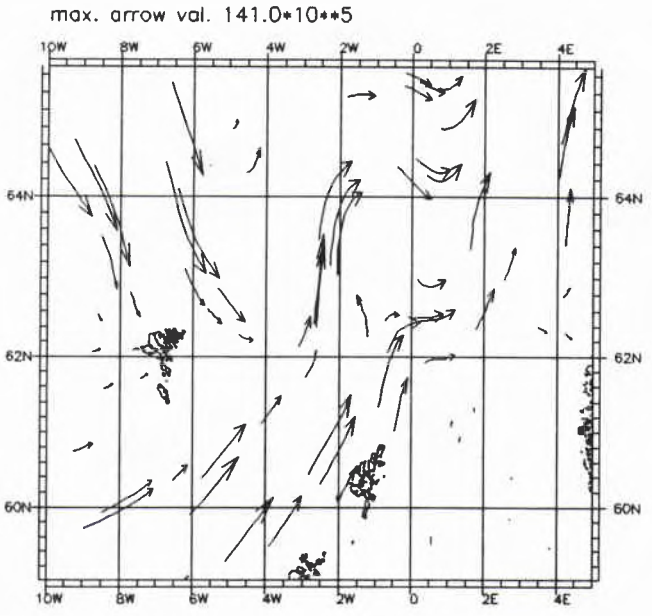

Fig. 5a. **The absolute velocities computed from the AIE data: Total transport (values are in cgs units).**

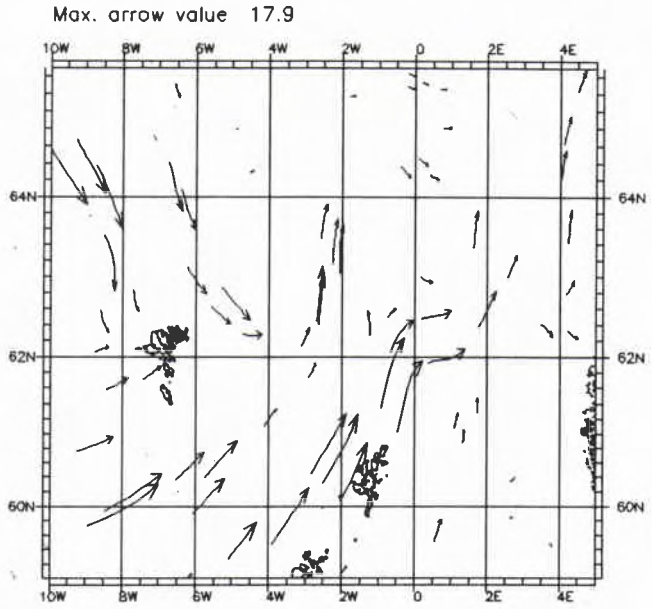

Fig. 5b. **The absolute velocities computed from the AIE data: Mean velocity (values are in cgs units).**

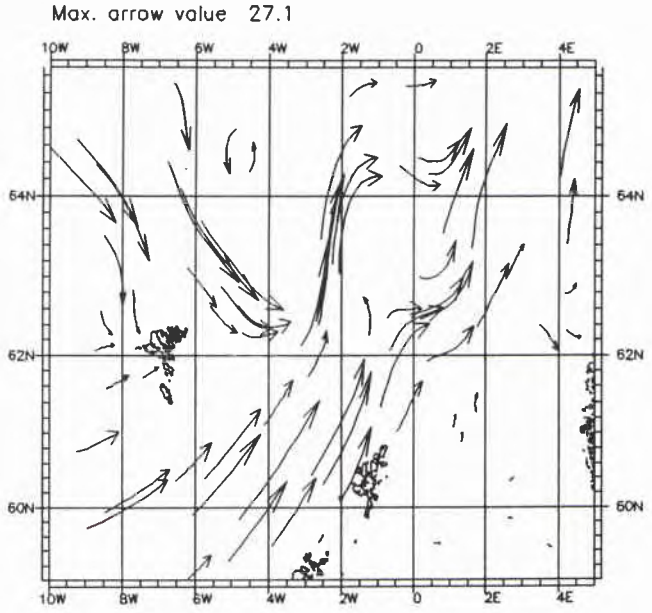

Fig. 5c. **The absolute velocities computed from the AIE data: Velocity field at 30 m depth (values are in cgs units).**

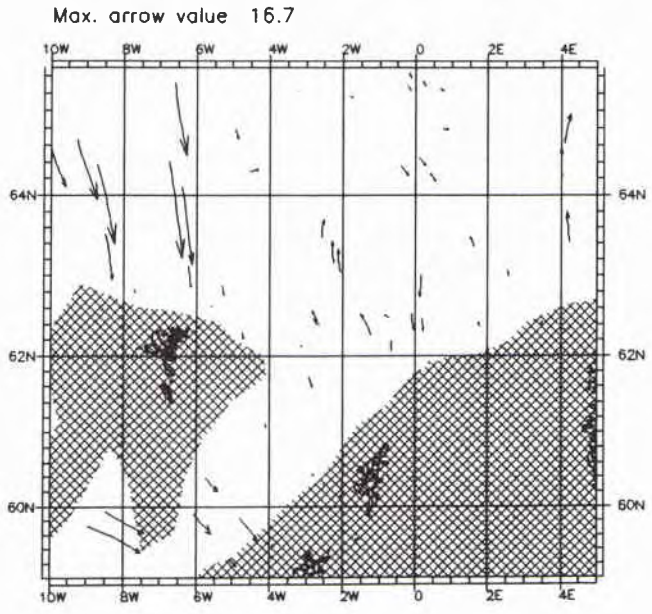

Fig. 5d. **The absolute velocities computed from the AIE data: Velocity field at 500 m depth (values are in cgs units).**

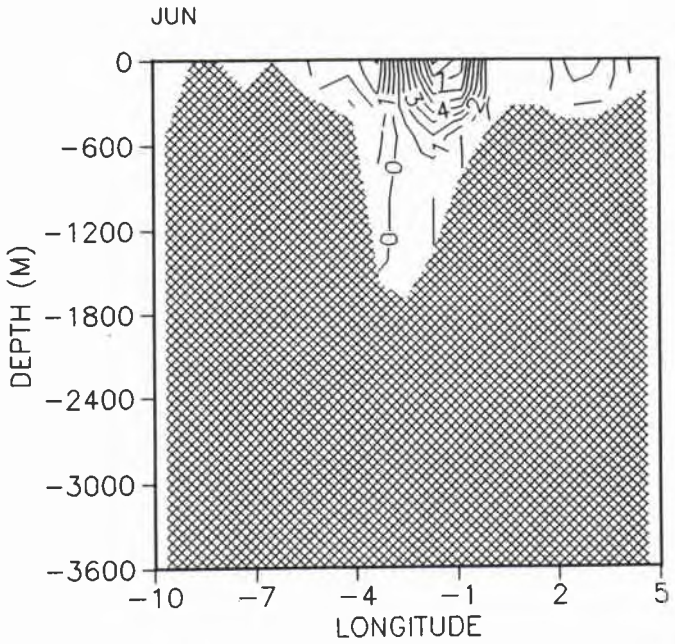

Fig. 6a. **The poleward velocity at 61.5°N during AIE (contour interval $\Delta V = 1$ cm/s^{-1}).**

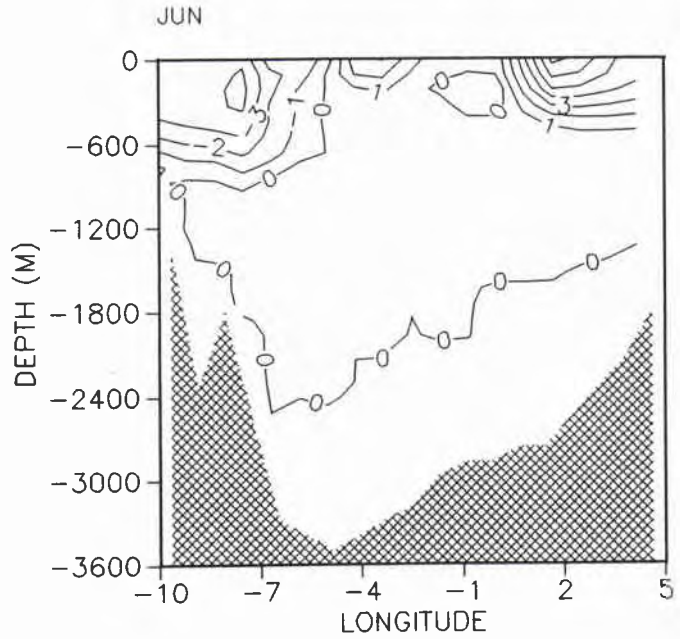

Fig. 6b. **The poleward velocity at 64°N during AIE (contour interval $\Delta V = 1$ cm/s^{-1}).**

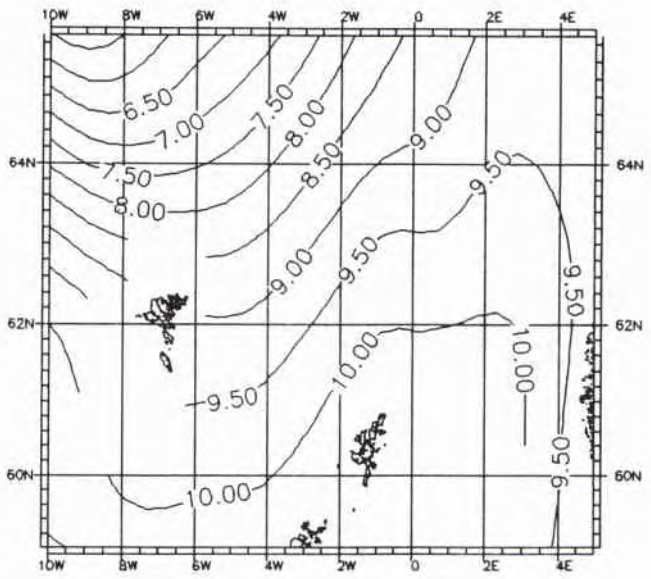

Fig. 7a. **The climatological constituent distributions at 30 m depth relative to AIE: Temperature (contour interval $\Delta T = 0.5°$).**

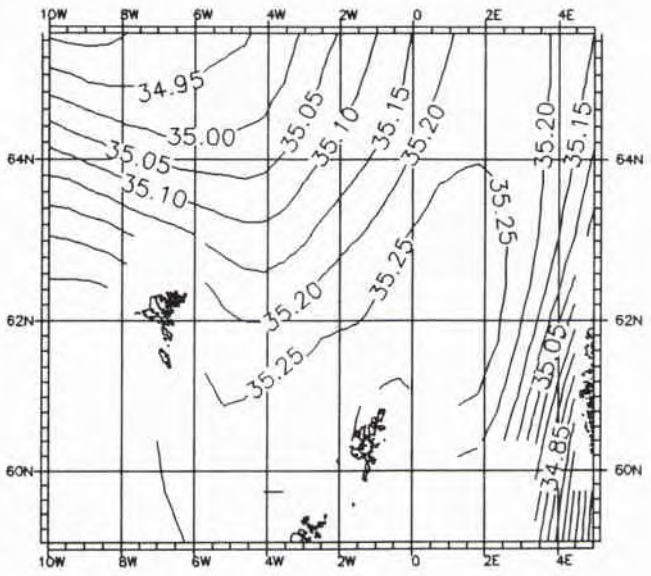

Fig. 7b. **The climatological constituent distributions at 30 m depth relative to AIE: Salinity (contour interval $\Delta S = 0.05$ ppt).**

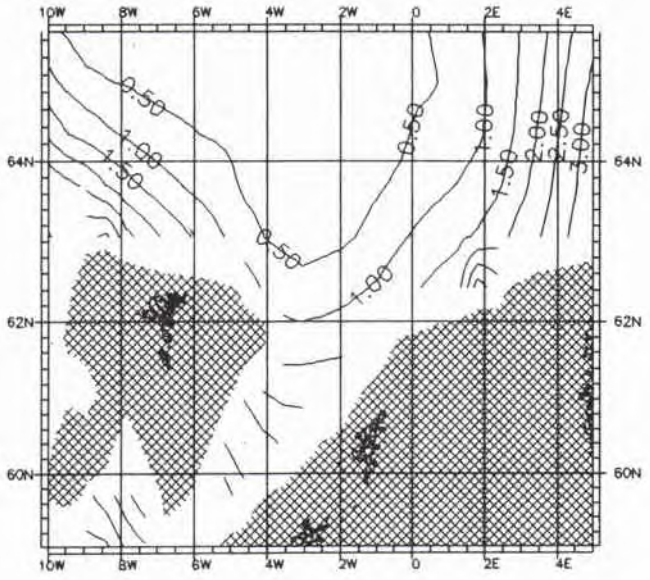

Fig. 8a. The climatological constituent distributions at 500 m depth relative to AIE: Temperature ($\Delta T = 0.5°$).

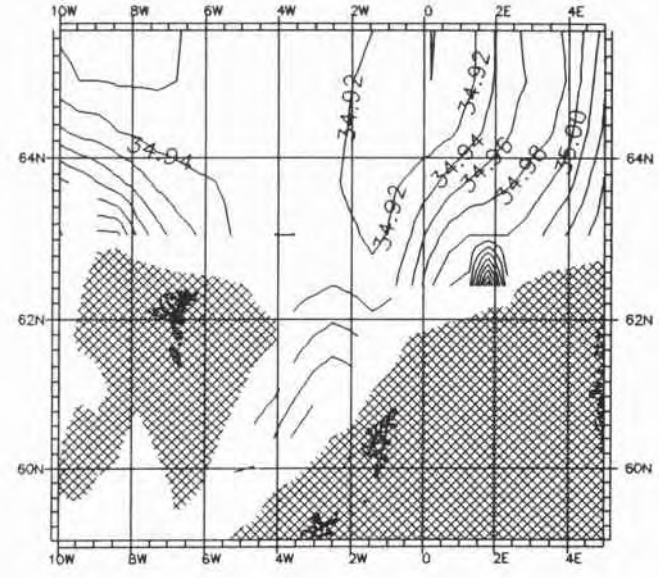

Fig. 8b. The climatological constituent distributions at 500 m depth relative to AIE: Salinity ($\Delta S = 0.02$ ppt).

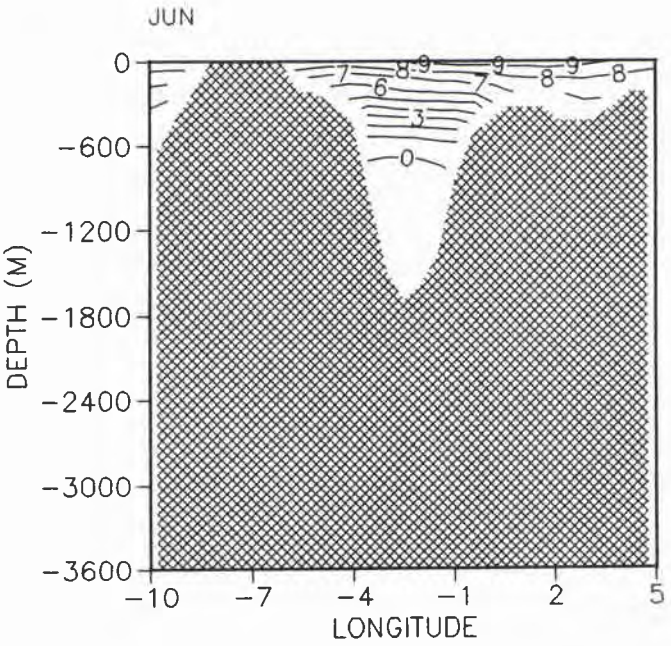

Fig. 9a. **Two climatological longitudinal section: Temperature at 61.5°N ($\Delta T = 1°$).**

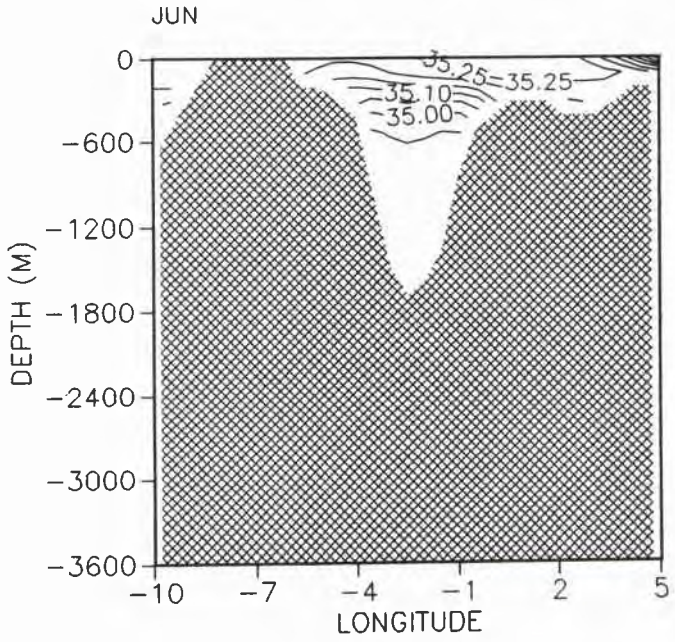

Fig. 9b. **Two climatological longitudinal section: Salinity at 61.5°N ($\Delta S = 0.05$ ppt).**

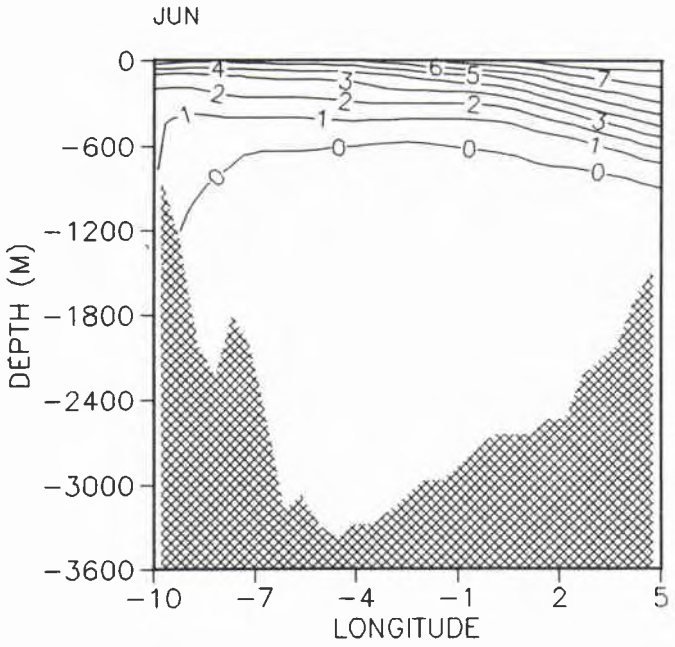

Fig. 9c. **Two climatological longitudinal section: Temperature at 64°N ($\Delta T = 1°$).**

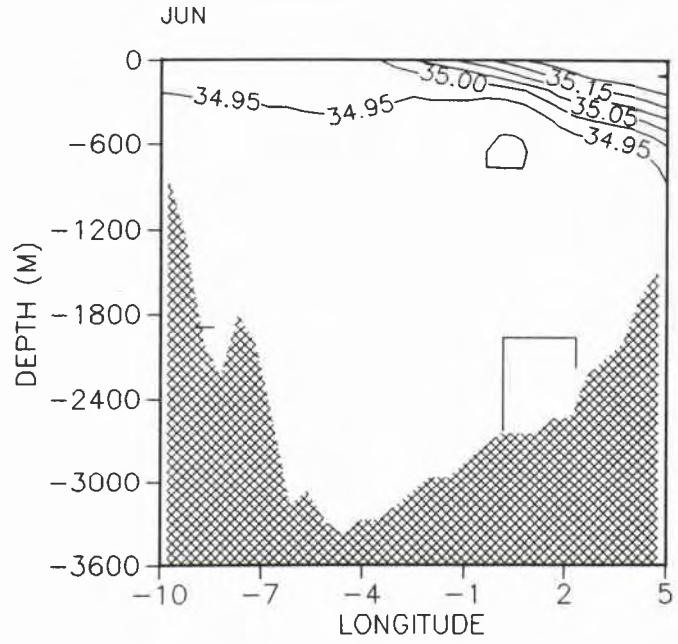

Fig. 9d. **Two climatological longitudinal section: Salinity at 64°N ($\Delta S = 0.05$ ppt).**

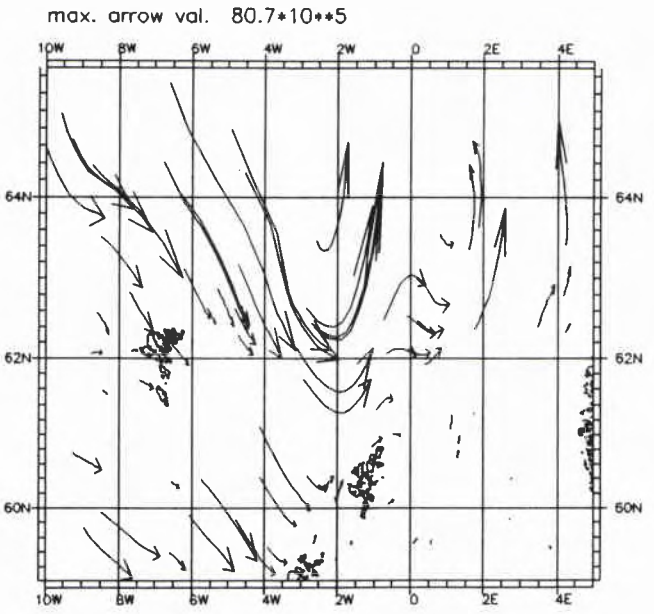

Fig. 10a. The absolute velocities computed from climatological data: Total transport (values are in cgs units).

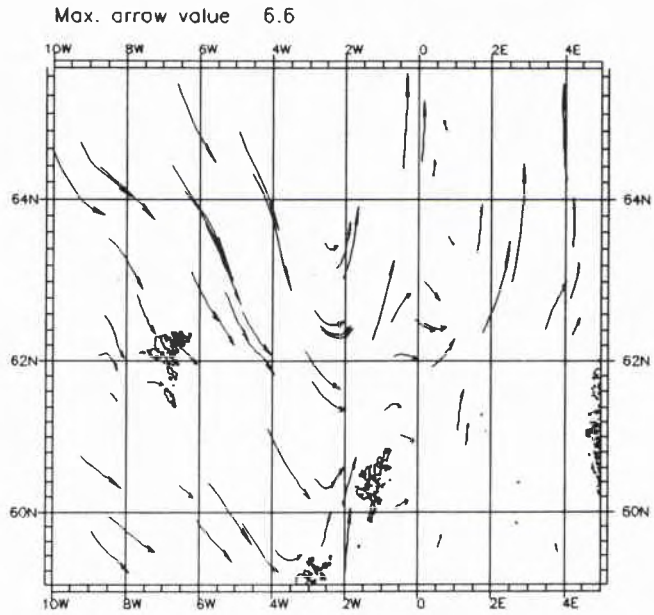

Fig. 10b. The absolute velocities computed from climatological data: Mean velocity (values are in cgs units).

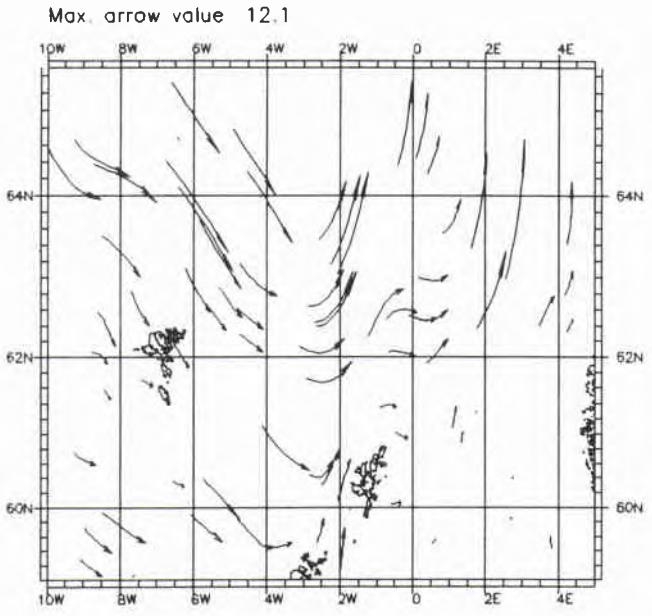

Fig. 10c. The absolute velocities computed from climatological data: Velocity field at 30 m depth (values are in cgs units).

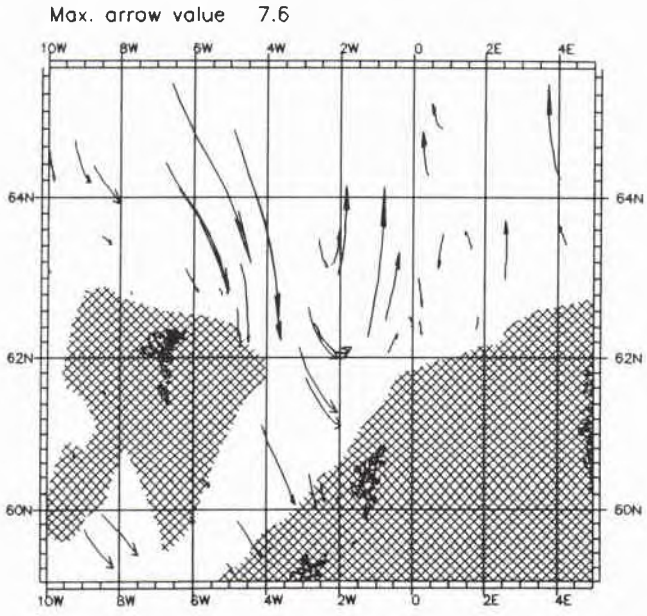

Fig. 10d. The absolute velocities computed from climatological data: Velocity field at 500 m depth (values are in cgs units).

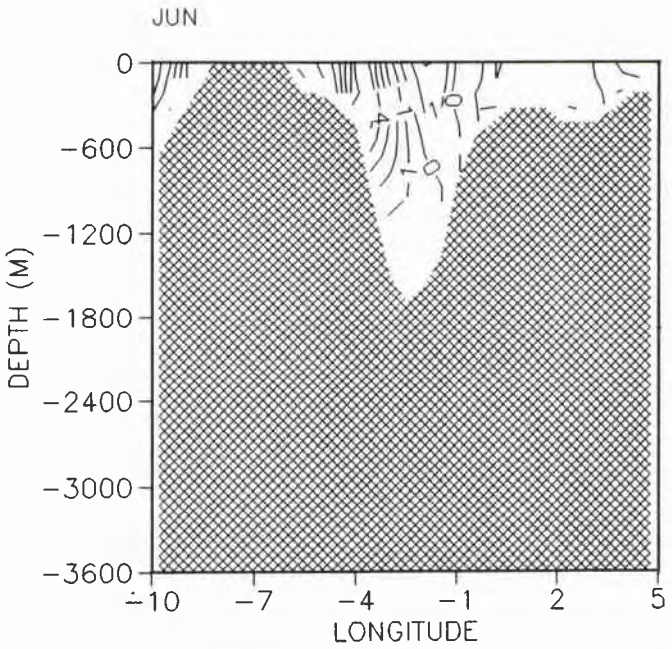

Fig. 11a. The poleward velocity at 61.5°N from climatological data (contour interval $\Delta V = 1$ cm/s^{-1}).

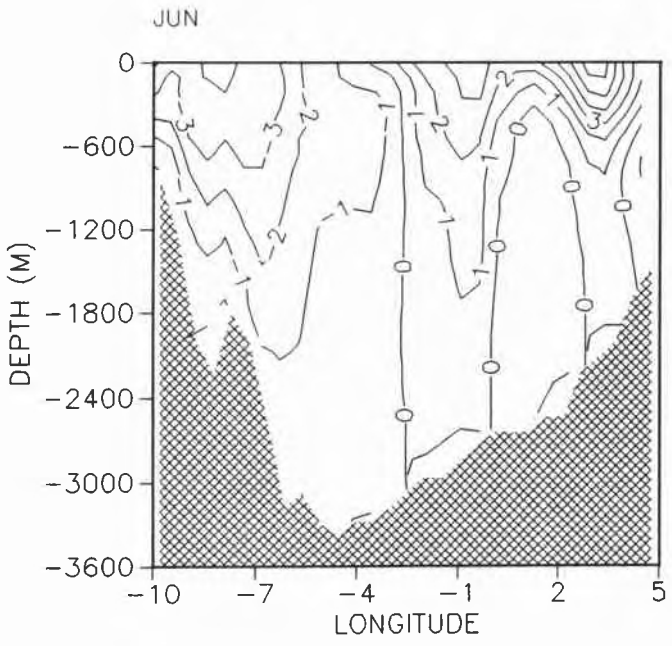

Fig. 11b. The poleward velocity at 64°N from climatological data (contour interval $\Delta V = 1$ cm/s^{-1}).

Report no. changed (Mar 2006): SR-155-UU

Initial Distribution for SR-155

Ministries of Defence	
JSPHQ Belgium	2
DND Canada	10
CHOD Denmark	8
MOD France	8
MOD Germany	15
MOD Greece	11
MOD Italy	10
MOD Netherlands	12
CHOD Norway	10
MOD Portugal	5
MOD Spain	2
MOD Turkey	5
MOD UK	20
SECDEF US	60
NATO Authorities	
Defence Planning Committee	3
NAMILCOM	2
SACLANT	3
SACLANTREPEUR	1
CINCWESTLANT/ COMOCEANLANT	1
COMSTRIKFLTANT	1
CINCIBERLANT	1
CINCEASTLANT	1
COMSUBACLANT	1
COMMAIREASTLANT	1
SACEUR	2
CINCNORTH	1
CINCSOUTH	1
COMNAVSOUTH	1
COMSTRIKFORSOUTH	1
COMEDCENT	1
COMMARAIRMED	1
CINCHAN	3
SCNR for SACLANTCEN	
SCNR Belgium	1
SCNR Canada	1
SCNR Denmark	1
SCNR Germany	1
SCNR Greece	1
SCNR Italy	1
SCNR Netherlands	1
SCNR Norway	1
SCNR Portugal	1
SCNR Turkey	1
SCNR UK	1
SCNR US	2
SECGEN Rep. SCNR	1
NAMILCOM Rep. SCNR	1
National Liaison Officers	
NLO Canada	1
NLO Denmark	1
NLO Germany	1
NLO Italy	1
NLO UK	1
NLO US	1
NLR to SACLANT	
NLR Belgium	1
NLR Canada	1
NLR Denmark	1
NLR Germany	1
NLR Greece	1
NLR Italy	1
NLR Netherlands	1
NLR Norway	1
NLR Portugal	1
NLR Turkey	1
NLR UK	1
Total external distribution	236
SACLANTCEN Library	10
Stock	34
Total number of copies	280